RESEARCH ON THE INFLUENCE OF VENTURI AERATOR CONFIGURATION ON OXYGEN ABSORPTION PERFORMANCE
/
文丘里增氧器结构参数对吸氧性能的影响研究

Longlong REN [1,2,3*)], Qingfu GONG[1,2)], Zhenxiang JING [1)], Xiang HAN [1,2)], Ang GAO [1,2)], Yuepeng SONG [1,2,3*)]
[1)] Shandong Agricultural University, College of Mechanical and Electrical Engineering / China;
[2)] Shandong Provincial Engineering Laboratory of Agricultural Equipment Intelligence / China;
[3)] Shandong Provincial Key Laboratory of Horticultural Machinery and Equipment/ China
Tel:15550851588; E-mail: renlonglong123@126.com; uptonsong@163.com
DOI: https://doi.org/10.35633/inmateh-74-25

Keywords: *Venturi oxygen; Oxygen absorption performance; Numerical simulation; Experimental verification*

ABSTRACT
In order to address the issue of low oxygen stress caused by crops in traditional facility agriculture, this paper designed and optimized a venturi aeration device to enhance the oxygen content in the rhizosphere of crops in facility orchards. With the assistance of Comsol software, visual analysis of the flow field was conducted using Computational Fluid Dynamics (CFD) technology, exploring the impact of throat deviation and air inlet positioning on the suction efficiency of the aerator. The results indicated that the eccentric venturi configuration significantly improved suction efficiency. Moreover, positioning the air inlet on the contracted side of the eccentric venturi throat increased suction efficiency by 12.7%. Analysis of flow field characteristics of various venturi aerator configurations identified key factors influencing suction capacity, including throat flow velocity, vortex morphology in the diffuser section, and distribution of turbulent energy within the aerator. To validate the accuracy of the numerical simulations, an oxygen absorption performance testing apparatus was constructed and simulation results were compared with experimental data. The analysis revealed an error range between the two results of 1.67% to 7.74%, confirming the reliability of the simulations. This study has provided a theoretical foundation and technical methodology for the structural design and optimization of venturi aerators.

摘要
为了解决传统设施农业中对作物造成的低氧胁迫问题，本文设计并优化了一种文丘里增氧装置，旨在提高设施果园作物根际的氧含量。借助 Comsol 软件，基于流体动力学（CFD）技术进行流场的可视化分析，并探究喉管的偏移程度及进气口的位置对增氧器的吸气效率的影响。研究结果表明，偏心文丘里配置能显著提升吸气效率。此外，将进气口设置在偏心文丘里管喉管的收缩端一侧，能够使吸气效率提高 12.7%。通过分析文丘里增氧器不同构型的流场特性，得到影响吸气量的关键因素主要包括喉管处的流速、扩散段的漩涡形态及增氧器内部的湍流能量分布情况。为了验证数值模拟仿真的准确性，构建了一套吸氧性能测试装置，并将仿真结果与试验结果进行了对比，结果比较分析表明二者之间的误差范围介于 1.67%至 7.74%，验证了仿真结果的可靠性。该研究为文丘里增氧装置的结构设计与优化提供了理论依据和技术方法。

INTRODUCTION
In recent years, with the growth of global population and the acceleration of urbanization, facility agriculture, as an efficient agricultural production mode, has attracted more and more attention and promotion *(Ding et al., 2023; Li et al., 2021)*. However, due to the long time required for drip irrigation, hypoxia stress often occurs in the rhizosphere of crops, which greatly limits the improvement of crop yield and quality *(Zahra et al., 2021; Zhu et al., 2020)*. Root hypoxia not only limits the absorption of water and nutrients by plants *(Salvatierra et al., 2020)*, but also hinders the metabolic process of crops, thereby inhibiting their growth and development *(León et al., 2021; Kapoor et al., 2022)*.

Venturi aerator is widely used in facility agriculture as an aerator. Through the design of specific structural parameters, it can effectively increase the oxygen concentration in the root area and promote the healthy growth of crops. The oxygenation effect of the oxygenation device directly affects the oxygen content of the water body during irrigation and the effect on soil aeration. Therefore, it is particularly important to optimize the design of the oxygenation device.

In the early 21st century, the United States developed an innovative irrigation method called AUDI technology, which improves the gas environment of roots by directly transporting oxygen to plant roots, thereby increasing crop yield *(Xie et al., 2019)*. The large-scale farmland irrigation system based on computer control developed by Eldar-Shany Automatic Control Technology is considered to be one of the cutting-edge control systems in the field of intelligent agriculture *(He et al., 2021)*. Li Yunkai et al. from China Agricultural University added ultra-micron bubble generators to the water and fertilizer integration device to increase the oxygen content of the water body *(Li et al., 2015)*. Liu Jun et al. from Jiangsu Academy of Agricultural Sciences optimized and designed a new type of U-shaped structure substrate tank to increase the oxygen content of irrigation water *(Liu et al., 2014)*. Fan Xingke et al. developed an eccentric venturi aerator, and found that its performance exceeded the traditional coaxial design *(Fan et al., 2014)*. In addition, Wang Haitao et al. compared the flow field distribution of the same axis and the eccentric venturi through the finite element analysis method, and revealed that the eccentric venturi has less head loss due to the smaller conflict of multi-directional velocity in the throat, which makes it more efficient *(Wang et al., 2018)*.

At present, a variety of venturi aerator irrigation devices have been developed at home and abroad, but there are significant differences in the effect and application of these devices. In addition, the research on the specific influence mechanism of different structural parameters on the aeration performance of venturi aerator is relatively insufficient. Based on this, according to the agronomic requirements of aerated irrigation in facility agriculture, this paper deeply discusses the specific influence of the key structural parameters of venturi aerator on its oxygen absorption performance in the integrated water and fertilizer system of facility agriculture, and optimizes the design of venturi aerator, which is of great significance for improving agricultural production efficiency and promoting crop growth.

MATERIALS AND METHODS

Structural model

Venturi aerator is a common aeration device used to inject air into water to provide oxygen *(Yagci et al., 2020)*. Its theoretical basis is Bernoulli equation. The general form of Bernoulli equation is as follows:

$$P + \frac{1}{2}\rho v^2 + \rho g h = c \quad (1)$$

In the above formula, P is the hydrostatic pressure; ρ is the fluid density; v is the fluid velocity; g is the acceleration of gravity; h is the height of the fluid at this point; c is a constant.

Based on the venturi effect in hydrodynamics, a venturi aerator is designed to increase oxygen content in water *(Yao et al., 2022)*. This device guides the water flow through a narrow channel inside, thereby generating a low-pressure environment in the local area. In the narrow part of the venturi aerator, this low-pressure environment causes the surrounding air to be inhaled and mixed with the water flow, thereby increasing the oxygen content in the water body. The conventional coaxial venturi structure is shown in Fig. 1.

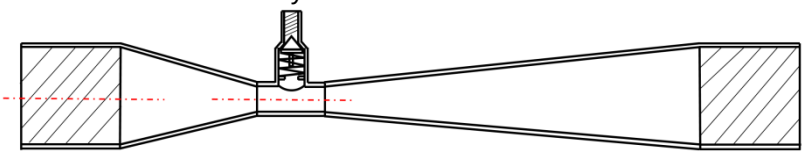

Fig.1 - The conventional coaxial venturi structure diagram

By optimizing the design of the venturi aerator, especially adjusting its internal structure, the flow field characteristics during operation can be significantly improved, thereby improving the suction efficiency and overall performance of the aerator. According to the agronomic requirements and existing problems of aerated irrigation in facility agriculture *(Wen et al., 2023)*, the structure of venturi aerator was optimized, and the concentric structure was optimized as an eccentric structure, as shown in figure 2.

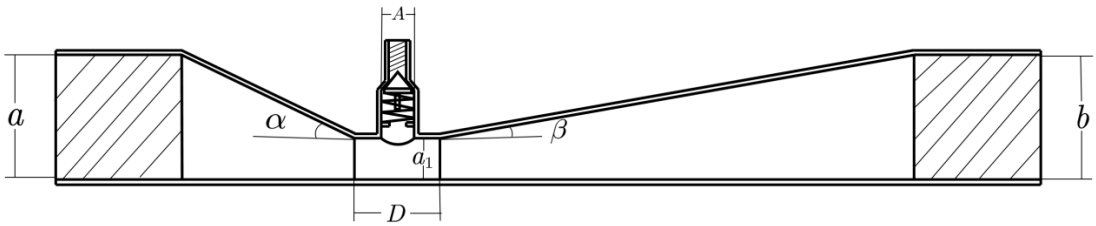

Fig. 2 - Structure diagram of eccentric venturi aerator

a. The diameter of inlet straight pipe section; b. The diameter of outlet straight pipe section; α. The angle of contraction section; β. The angle of diffusion section L; a_1. Throat diameter; D. Throat length; A. Inlet diameter

The basic structure of eccentric venturi aerator includes six main parts: inlet straight pipe section, contraction section, throat pipe, diffusion section, outlet straight pipe section and suction pipe. The key parameters include contraction section angle α, diffusion section angle β, throat diameter a_1, throat diameter-length ratio λ ($\lambda = D/a_1$), throat contraction ratio γ ($\gamma = a_1/a$), throat length D and inlet diameter A. The difference of these parameters will significantly affect the working performance and efficiency of venturi aerator. Aiming at the offset distance S of the throat relative to the central axis of the overall structure and the distance L from the inlet to the contraction end of the throat, a series of models with different parameters were constructed to carry out experimental and numerical simulation analysis. After dividing the distance parameters, five different S values were set, which were S1 (0 mm), S2 (2.5 mm), S3 (5 mm), S4 (7.5 mm) and S5 (10 mm). And five different L values, L1 (5 mm), L2 (7.5 mm), L3 (10 mm), L4 (12.5 mm) and L5 (15 mm). The specific structural parameters of the venturi aerator are shown in Table 1.

Table 1

Structure parameters of the eccentric venturi aerator

Structure name	Numerical value
Diameter of inlet straight pipe section (mm)	30
Outlet straight pipe diameter (mm)	30
Angle of contraction segment（°）	25
Diffusion section angle（°）	8
Throat diameter (mm)	10
Throat pipe length (mm)	20

Numerical simulation

When using Computational Fluid Dynamics (CFD) technology to visualize the flow field, a three-dimensional model is first created by SolidWorks, as shown in Figure 3, and Comsol 6.1 is used for meshing for subsequent analysis. The model meshing is shown in Figure 4. In order to ensure the calculation accuracy while reducing the consumption of computing resources, it is necessary to perform mesh independence verification to determine the optimal mesh size.

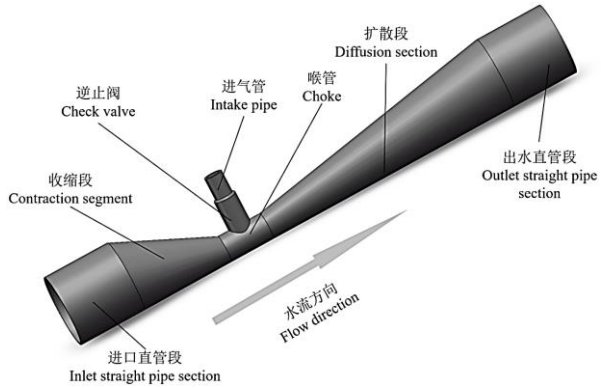

Fig. 3 - 3D model of eccentric venturi aerator

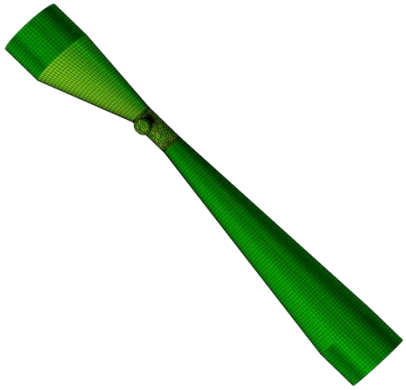

Fig. 4 - Model grid division diagram

According to the research of Zhang et al. *(Zhang et al., 2021)*, the simulation accuracy is mainly affected by the mesh size, and the correlation with the calculation condition is low. Based on this, grid independence verification was carried out under specific working conditions (inlet flow rate was 1 m/s, outlet and inlet pressure were both 0 MPa), and the change rate of fertilizer suction flow was used as the test index to explore the relationship between the number of grids and the change rate of fertilizer suction flow. The results show that when the difference between the calculation results is less than 0.5 %, the grid density has little effect on the accuracy of the calculation results. Therefore, the grid configuration can be regarded as a suitable computational grid *(Xing et al., 2021)*.

In order to further optimize the calculation accuracy of the model and reduce the calculation cost, a combination of hexahedral and tetrahedral grids is used for meshing. Tetrahedral meshes are used in the throat area to accurately capture the complex flow phenomena of gas-liquid mixing, while hexahedral meshes are used in other areas of the model to improve the computational efficiency and the accuracy of flow field analysis. The curve of the relationship between the maximum grid size and the change of air flow velocity obtained by simulation calculation is shown in figure 5. After comprehensive consideration, it is finally determined that the model shows the best analysis effect under the condition that the maximum grid size is 0.0016 m.

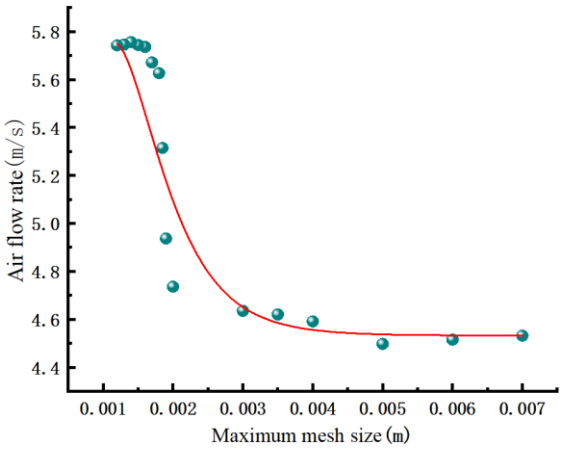

Fig. 5 - Curve of the relationship between the maximum grid size and the variation of air flow velocity

RESULTS

Analysis of the influence of different configurations of venturi aerator

In the study of structural optimization of venturi aerator, two key structural parameters S (the offset distance of the throat relative to the central axis of the overall structure) and L (the distance from the inlet to the contraction end of the throat) need to be considered comprehensively. The S5 venturi aerator designed in this paper is a prototype design proposed by Kong Lingyang et al. *(Kong et al., 2013)*. The design is characterized by a downward bias of the throat and a smooth wall away from the suction side. Based on this prototype, the L parameters are optimized by adjusting the values to obtain the best structural configuration. Accordingly, the venturi aerator design can be summarized into nine different combinations, namely *S1L1*, *S2L1*, *S3L1*, *S4L1*, *S5L1*, *S5L2*, *S5L3*, *S5L4* and *S5L5*. The design explores whether different combination configurations will affect the suction efficiency of the venturi tube, and further explores its influence principle. This paper will discuss the specific effects of these combined configurations on the performance of venturi aerators through in-depth analysis.

The fluid dynamics simulation analysis of nine different configurations of venturi aerators was carried out to observe their air suction performance under uniform flow rate conditions (1 m/s). CFD is used to simulate the flow characteristics of each configuration, and the corresponding air suction flow rate is combined. The results are presented in figure 6 in the form of point-line diagram. It can be seen from the figure that the simulated maximum air suction flow rate reaches 5.73 m/s, and the structure with this value is *S5L1*.

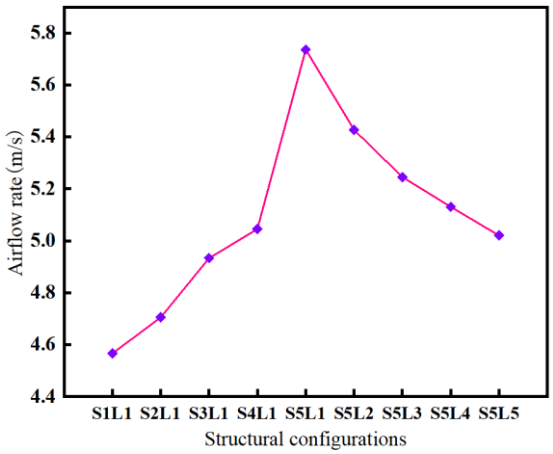

Fig. 6 - The influence of throat position on air flow velocity

It can be seen from Fig. 6 that under the condition of fixed inlet relative position (L), with the increase of throat deflection (S), the air velocity increases obviously and reaches the peak at $S5$. In the case of selected S5 skewness, it is observed that the air flow rate gradually decreases with the increase of the relative position (L) of the inlet, and the rate of flow rate decrease gradually slows down. After examining nine different combinations of relative position and skewness of inlets, it is found that the structure of *S5L1* combination produces the highest air flow velocity, which is 20.2 % higher than that of *S1L1* combination. This result shows that the configuration of the venturi aerator has a significant effect on the air velocity.

In describing the performance parameters of venturi aerator, the gas-liquid ratio (the ratio of the liquid volume flow rate of the venturi aerator to the volume flow rate of the inhaled air) is usually used to measure the aerator 's suction capacity. The formula is:

$$\varepsilon = \frac{Q_V}{Q_W} \tag{2}$$

In the above formula, ε is the gas-liquid ratio; Q_V is the volume flow rate of air; Q_W is the liquid volume flow rate.

As shown in Figure 7, the relationship between the gas-liquid ratio and the venturi configuration follows the same trend as the previous analysis data. With the increase of the skewness S, the gas-liquid ratio gradually increases, and reaches the maximum value of 0.408 at S5. On the contrary, with the increase of the relative position L of the inlet, the gas-liquid ratio shows a gradual downward trend, and the gas-liquid ratio is the highest at $L1$. When comparing 9 different configurations of venturi aerators, it was found that the venturi aerator with $S5L1$ structure had the highest gas-liquid ratio, which was 12.7 % higher than that of $S5L5$.

Through the detailed analysis of the changes of structural parameters S and L, it can be concluded that the increase of skewness S has a significant positive effect on the air intake efficiency of the venturi aerator, while the increase of the relative position L of the inlet has a negative effect on the air intake efficiency. Therefore, under the structural configuration of $S5L1$, the overall suction efficiency of the venturi aerator is optimal.

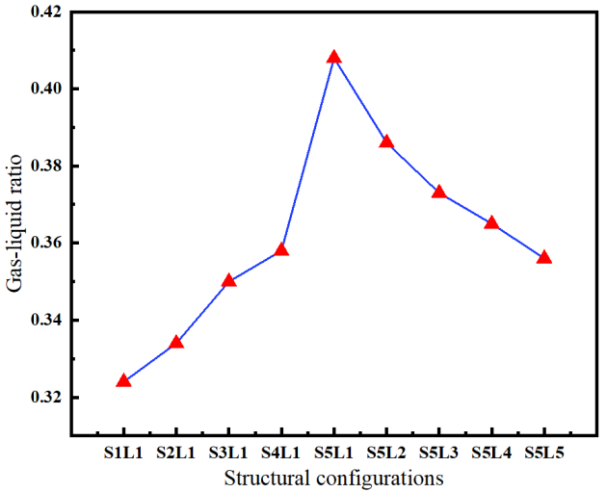

Fig. 7 - Effect of throat position on gas-liquid ratio

Analysis of the influence of inlet velocity of S5L1 venturi aerator on suction volume

Fig.8 shows the relationship between the water flow velocity and the suction gas flow velocity in the S5L1 venturi aerator and its corresponding fitting curve. It can be seen from the diagram that with the increase of water flow velocity, the gas flow velocity also increases accordingly. This phenomenon is consistent with the prediction of Bernoulli 's principle, that is, the increase of fluid velocity will reduce its own pressure, and then increase the pressure difference at the inlet, and finally increase the gas velocity at the inlet.

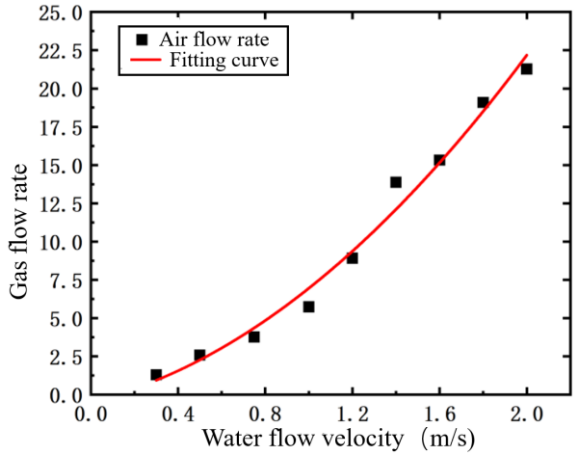

Fig. 8 - Influence of water velocity on air velocity

With the increase of water flow velocity, the gas suction volume at the inlet shows an increasing trend. However, an increase in the velocity of the water flow can also lead to an increase in the flow rate of the water. These two factors work together on the suction efficiency of the aerator. According to the data analysis shown in Fig.9, it can be seen that the gas-liquid ratio gradually increases with the increase of water flow velocity. In the area where the water flow velocity is lower than 0.8 m/s, the growth rate of gas-liquid ratio is low and fluctuates to some extent. When the water flow velocity is in the range of 0.8 m/s to 1 m/s, the growth of the gas-liquid ratio is significantly accelerated, and after exceeding 1.4 m/s, the growth rate slows down and gradually stabilizes. Within the specified range of flow rates in the simulation calculations, it is evident that increasing the inlet flow rate results in a corresponding increase in the inlet suction flow rate. Moreover, a notable linear correlation exists between the water flow rate and the gas flow rate at the inlet.

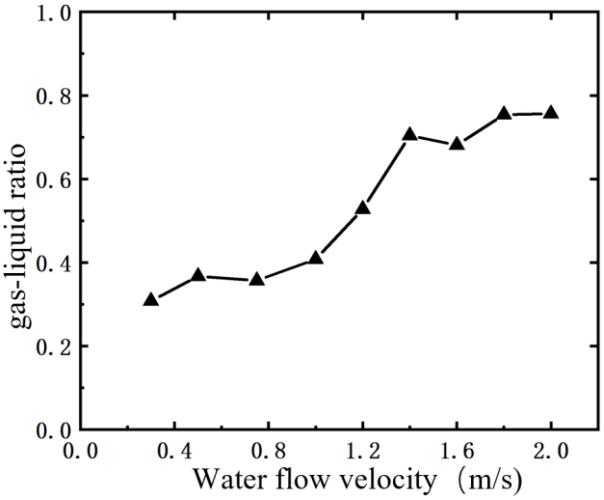

Fig. 9 - Influence of water velocity on gas-liquid ratio

Experimental verification

The test sample was printed by a 3D printer with an accuracy of 0.5 mm, and the printing material was high toughness resin. Figure 10 is the solid model of S5L1 venturi aerator. The fluid is injected into the aerator through the left inlet. When it passes through the contraction area, the flow rate increases and the pressure decreases. When it flows through the throat section, a negative pressure is generated, and the external gas can be sucked into the aerator through the inlet. Subsequently, the gas-liquid two-phase mixture is discharged from the outlet to achieve the purpose of gas-liquid mixing.

Fig. 10 - Physical drawing of S5L1 venturi aerator

To ensure precise measurement of the flow characteristics of the *S5L1* venturi aerator, a turbine flowmeter was employed for data collection in this study, offering a measurement range of 9 to 100 L/min. When assessing air flow velocity, the gas flow parameters were acquired using a glass rotor flowmeter. Based on simulation outcomes, a glass rotor flowmeter with a range of 6 to 45 L/min was selected to encompass the required measurement scope for the experiment.

In order to verify the accuracy of the numerical simulation results, a suction performance test system was designed and built, as shown in Figure 11. The test platform uses a submersible pump to provide a pressure water source. The submersible pump is equipped with a flow regulation function. In the test, the water flow through the venturi aerator is controlled by adjusting the operating state of the submersible pump. The turbine flowmeter is connected in series behind the submersible pump to read the water flow through the aerator in real time. The inlet end of the venturi tube is externally connected with the glass rotor flowmeter. The inlet end of the flowmeter leads to the external environment, and the outlet end is connected with the inlet port of the aerator.

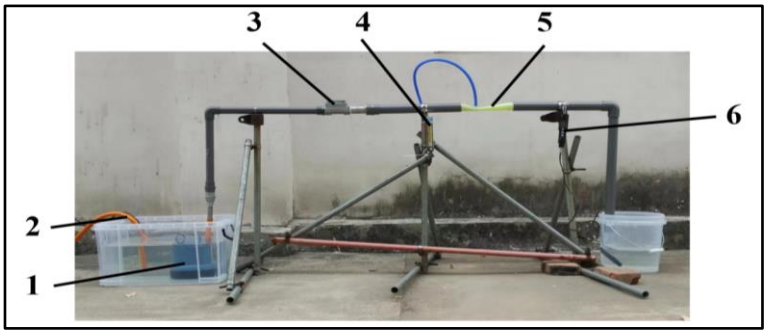

Fig. 11 - Inspiratory performance test device

1. Submersible pump; 2. Permanent water; 3. Turbine flowmeter; 4. Glass rotor flow meter; 5. Venturi aerator type S5L1; 6. Dissolved oxygen measuring instrument

During the experimental operation, the flow rate is gradually increased from low to high, and after each adjustment of the flow rate, the readings of the turbine flowmeter and the glass rotor flowmeter in the stable state are recorded respectively to obtain accurate flow data. According to the test device, the simulation reliability verification test was carried out. The test explored the relationship between the inlet flow rate and the air flow rate by adjusting the inlet flow rate of the venturi aerator. Figure 12 shows the trend and change curve of the simulated value and the experimental value. The experimental results show that the trend of the simulation data is basically the same as that of the experimental data, and the error range between the two is between 1.67 % and 7.74 %, which is within the acceptable error range. In addition, the data comparison verifies the accuracy and applicability of the computational simulation model, which proves that it can be effectively used to explain the optimization results.

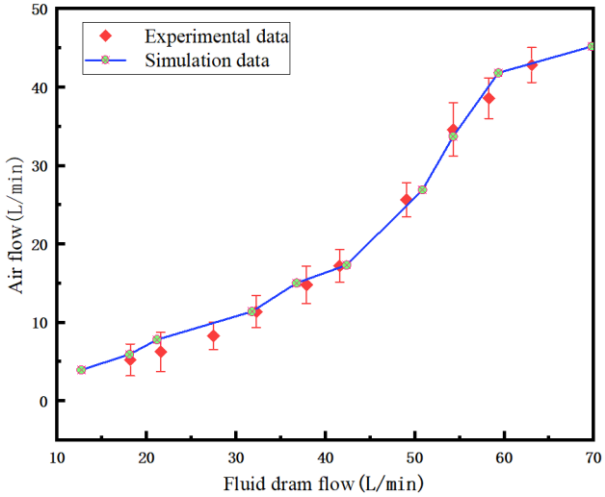

Fig. 12 - Comparison of simulation data with experimental data

Analysis of velocity characteristics of throat pipe

Figure 13 is the distribution of flow velocity characteristics of venturi aerators with different configurations. On the premise of the same working environment, according to the Bernoulli principle, it can be observed that in the throat area, the increase of the flow rate leads to the decrease of the negative pressure near the inlet area, which improves the suction efficiency and reduces the energy loss. With the gradual downward movement of the throat position from $S1$ to $S5$, the flow rate of the throat shows an increasing trend, which reaches the maximum at the $S5$ position. When the position of the throat is kept unchanged at $S5$, when the position of the air inlet gradually moves from $L1$ to $L5$, the flow velocity of the throat shows a decreasing change, which is consistent with the previous experimental results of the inspiratory capacity. Through the velocity distribution map, it can be further observed that when the liquid flows through the inlet, the velocity increases obliquely downward. This phenomenon is caused by the external air introduced by the inlet above the throat. The mixing of the air and the water flow leads to the increase of the volume of the mixed fluid, which causes the increase of the flow rate. At the same time, because the air enters the throat along the normal direction of the air inlet, the flow velocity at the throat shows an oblique downward trend due to the influence of the water flow to the right side.

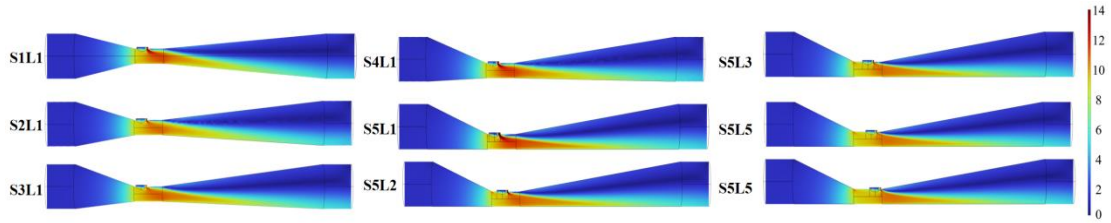

Fig. 13 - Distribution of velocity characteristics of venturi aerator

Vortex characteristics analysis

In order to accurately describe the position of the vortex center, this paper processes each vortex simulation result image. A plane rectangular coordinate system is established on the non-diffusion side of the outlet pipe, and this side is used as the coordinate origin (O). The X axis of the coordinate system extends along the inverse direction of the water flow, while the Y axis is vertical upward. In this way, the geometric characteristics of the vortex can be analyzed more clearly, as shown in Fig.14.

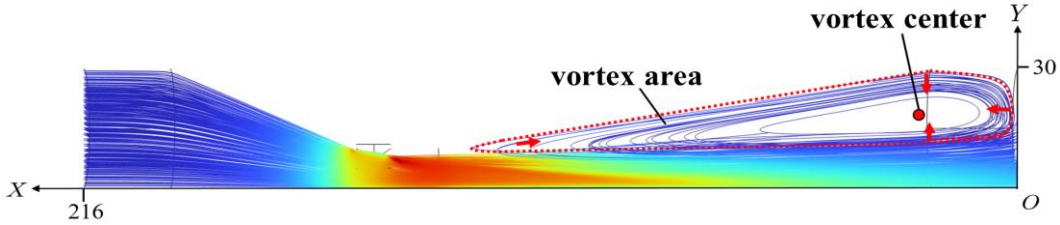

Fig. 14 - Location of vortex region and vortex center

The vortex boundary and the vortex center are processed to express the position of the vortex center on the coordinate system based on the plane right-angled coordinate system established above and measure its data loci marked on the X and Y axes of the coordinate system, and the processed vortex annotation map is shown in Figure 15.

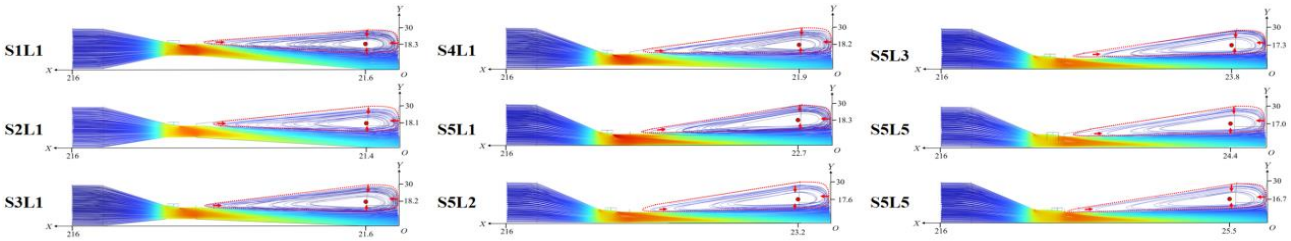

Fig. 15 - Vortexes of venturi aerators with different configurations

During the increment of the throat position from *S1* to *S5*, the change of the position of the vortex center is not significant and mainly moves irregularly in a small range. At the same time, the area of the vortex region shows a gradual reduction trend, in which the area of the vortex decreases by 256.5 mm² at the *S5* position compared with the *S1* position, which is a decrease of 20.9%. For the change of inlet position from *L1* to *L5*, the vortex center of the eccentric venturi oxygenator shifted in both X and Y axes. In this case, the vortex center was shifted to the left by 2.8 mm in the X-axis direction and downward by 1.6 mm in the Y-axis direction, with a combined shift distance of 3.2 mm downward from the left. In addition, there was a significant increase in the vortex area of 318.0 mm², which is an increase of 32.9%, as shown in Table 2.

Table 2

Vortex characteristics of the aerator at different intake positions

Venturi aerator configuration	Vortex center position		Vortex area (mm²)
	X-axis (mm)	Y-axis (mm)	
S1L1	21.6	18.3	1223.75
S2L1	21.4	18.1	1172.61
S3L1	21.6	18.2	1095.47
S4L1	21.9	18.2	1030.33
S5L1	22.7	18.3	967.2
S5L2	23.2	17.6	1013.8
S5L4	24.4	17.0	1171.4
S5L5	25.5	16.7	1285.2

Under the same working conditions, the vortex area of the venturi aerator under the *S5L1* configuration is the smallest, which leads to the relative increase of the effective area of the mainstream water flow. In addition, the vortex center of the *S5L1* venturi aerator is closest to the throat and the air inlet, resulting in the vortex area beginning to affect the working environment near the air inlet and hindering the inflow of gas. In contrast, the vortex area in the *S5L5* configuration is small and the vortex center is far away, so the interference to the working environment near the inlet is small, and the inflow of external air is hardly affected by the vortex. Compared with the *S5L1* configuration, the venturi aerator with the *S1L1* configuration has a more significant skewed flow due to the expansion of its diffusion section along the upper and lower directions. Therefore, it can be concluded that the mainstream area is mainly concentrated on the far side of the suction pipe, resulting in a large vortex in the diffusion section, which may affect the working efficiency of the aerator.

Analysis of turbulent kinetic energy distribution characteristics

Figure 16 is the turbulent kinetic energy distribution cloud map of the throat with different skewness S1-S5 and the inlet pipe at different positions of the throat *L1-L5*. Turbulent kinetic energy is an intuitive indicator to measure the degree of turbulence in the flow field. The higher turbulent kinetic energy reflects that the flow field is more complex, and the interaction, collision and mixing between the layers are more intense, resulting in an increase in local head loss *(Li et al., 2020)*. In the configuration of *S1-S4*, the venturi aerator shows obvious turbulent kinetic energy concentration in the throat area. With the increase of skewness *S*, the concentration of turbulent kinetic energy gradually decreases until the concentration of turbulent kinetic energy basically disappears in the *S5* state. This trend is due to the fact that different S values change the contraction structure at both ends of the venturi aerator, which affects the flow characteristics of the water flow into the throat and causes a significant concentration of turbulent kinetic energy in the throat area. For the case of *L1-L5*, the maximum turbulent kinetic energy appears in the middle region of the diffusion section. The reason is that with the increase of L value, the vortex area inside the venturi aerator expands accordingly, and the range and offset of the vortex area also increase. This causes the backflow in the vortex region to collide with the water flow in the mainstream region, making the flow pattern more chaotic and the turbulence intensity increased accordingly. In addition, when the air is sucked into the throat through the air inlet, it mixes with the water flow and collides violently in multiple directions, resulting in the disorder of the water flow in the throat, thereby increasing the turbulence intensity.

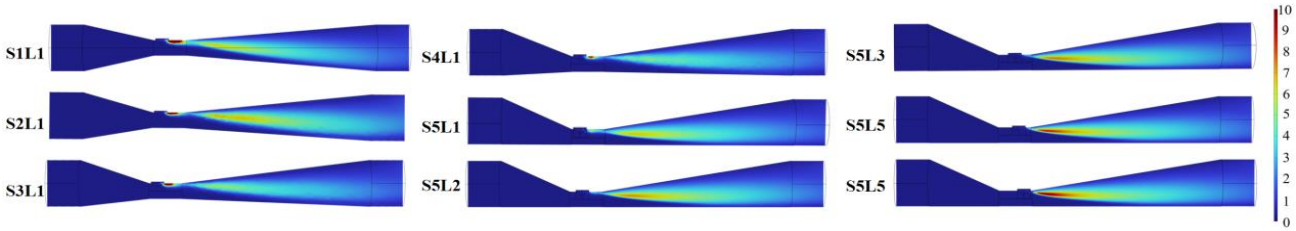

Fig. 16 - Distribution of turbulent kinetic energy of venturi aerators with different configurations

CONCLUSIONS

In this paper, the effects of the offset distance of the throat center and the relative position of different inlets at the throat on the suction performance and flow characteristics of the venturi aerator are compared and analyzed. The specific conclusions are as follows:

(1) Under normal working conditions, there is a good linear relationship between the deviation degree of the throat of the venturi aerator and the inspiratory efficiency. In addition, the relative position of the air inlet and the throat of the venturi aerator also shows a linear correlation with the inspiratory efficiency. When the venturi aerator is configured as S5L1 configuration, its inspiratory efficiency reaches the maximum.

(2) The simulation results of 9 configurations under the same working conditions show that the performance of S5L1 type is the best. Specifically, this configuration has the highest flow velocity at the throat, the smallest vortex area in the diffusion section, and the lowest turbulent kinetic energy. These three flow characteristics work together to make the S5L1 venturi aerator have the highest suction efficiency.

(3) Through the experimental study of the suction performance test bench and the calculation and analysis of the corresponding simulation model, this study reveals that there is a significant positive linear correlation between the liquid flow rate and the air flow rate in the venturi aerator. The variation trend of the simulation value is generally consistent with the actual value of the test, and the error range between the two is 1.67 % to 7.74 %.

ACKNOWLEDGEMENT

This work was sponsored by “Key R&D Program of Shandong Province, China” (2024TZXD045, 2024TZXD038); Shandong modern agricultural industrial technology system - special fund for fruit innovation team (SDAIT- 06 -12) - special fund for fruit facilities, machinery and equipment post.

REFERENCES

[1] Ding, Y.H., Zhang, Y.H., Sun, N., Fu, G.H., Lin, S., Chen, C. (2023). International experience and enlightenment of facility agriculture development in China (我国设施农业发展的国际经验与启示). *Jiangsu Agricultural Sciences*, Vol.51(16), pp.1-8.

[2] Fan, X.K., Kong, L.Y. (2014). The Selection of Venturi Injector in the Drip Irrigation System (滴灌系统中文丘里施肥器的选配方法). *Journal of Irrigation and Drainage*, Vol.33 (1), pp. 26-29.

[3] He, Q.H., Zheng, L., Chu, Y. H., Dou, Q.Q., Ci, W.L., Sun, Y.T. (2021). Research status and prospect of the head of fertigation system (水肥一体化系统首部研究现状与展望). *Chinese Journal of Agricultural Chemistry*, Vol.42 (1), pp. 122-129.

[4] Kapoor, R., Kumar, A., Sandal, S.K., Sharma, A., Raina, R., Thakur, K.S. (2022). Water and nutrient economy in vegetable crops through drip fertigation and mulching techniques: a review. *Journal of Plant Nutrition*, Vol.45(15), pp.2389-2403.

[5] Kong, L.Y., Fan, X.K. (2013). Experimental Study on Fertilizer Suction Performance of Venturi Injector (文丘里施肥器吸肥性能试验研究). *Water Saving Irrigation*, Vol.7, pp. 4-6.

[6] León, J., Castillo, M.C., Gayubas, B. (2021). The hypoxia-reoxygenation stress in plants. *Journal of experimental botany*, Vol.72(16), pp. 5841-5856.

[7] Li, H., Li, H., Huang, X.Q., Han, Q.B., Yuan, Y., Qi, B. (2020). Numerical and experimental study on the internal flow of the venturi injector. *Processes*, Vol.8(1), pp.64.

[8] Liu, J., Tao, J.P., Yan, J.M., Luo, K.Y., Han, J.M., Zheng, H.Q., Lv, X.L. (2014). A method of water, fertilizer and gas fertilization (一种水肥气施肥方法). CN103918393A.

[9] Li, W.F., Lin, F.L., Xiang, J.L., Xu, Q.Y., Li, H.P. (2021). Development Status and Countermeasures of Facility Agriculture (浅析设施农业发展现状及对策). *Guangdong Sericulture*, Vol.55(03), pp.12-15.

[10] Li, Y.K., Liu, X.J., Xu, F.P., Wang, X.R., Zhang, Q.L., Jia, R.Q. (2015). A water-fertilizer-gas integrated drip irrigation system and drip irrigation method (一种水肥气一体化滴灌系统及滴灌方法). CN103141206B.

[11] Salvatierra, A., Toro, G., Mateluna, P., Opazo, I., Ortiz, M., Pimentel, P. (2020). Keep calm and survive: Adaptation strategies to energy crisis in fruit trees under root hypoxia. *Plants*, Vol.9(9), pp.1108.

[12] Wang, H.T., Wang, J.D., Yang, B., Mo, Y. (2018). Numerical simulation of Venturi injector with non-axis-symmetric structure (非对称结构文丘里施肥器数值模拟). *Journal of Drainage and Irrigation Machinery Engineering*, Vol.36(11), pp. 1098-1103.

[13] Wen, H.Y., Yu, Z.Z., Wang, C., Zhang, D.M., Wang, H.X., Zou, H. F. (2023). Analysis on the Research Status and Development Trend of Aerobic Irrigation Technology (增氧灌溉技术研究现状与智能化发展趋势分析). *Journal of Agricultural Mechanization Research*, Vol.45(3), pp.1-7.

[14] Xie, P.J., Zhang, Y.B. (2019). Development and application of green and efficient water-fertilizer-gas irrigation system (绿色高效水肥气灌溉系统研发与应用). *Southern Agriculture*, Vol.13(31), pp.77-80.

[15] Xing, S.B., Wang, Z.H., Zhang, J.Z., Liu, N.N., Zhou, B. (2021). Simulation and verification of hydraulic performance and energy dissipation mechanism of perforated drip irrigation emitters [J]. *Water*, Vol.13(2), 171.

[16] Yagci, A.E., Unsal, M., Ercan, B. (2020). Investigation the aeration performance of a new aerator: Venturi conduit. *Fresenius Environmental Bulletin*, Vol.29(2), pp.917-930.

[17] Yao, N.Z., Wang, H., Wang, B., Wang, X.S. (2022). Venturi-effect rotating concentrators and nonreciprocity characteristics based on transformation hydrodynamics (基于变换流体动力学的文丘里效应旋聚器的设计与非互易特性研究). *Acta Phys Sin*, Vol.71(10), pp.104701.

[18] Zahra, N., Hafeez, M.B., Shaukat, K., Wahid, A., Hussain, S., Naseer, R., Raza, A., Iqbal, S., Farooq, M. (2021). Hypoxia and Anoxia Stress: Plant responses and tolerance mechanisms. *Journal of Agronomy and Crop Science*, Vol.207(2), pp.249-284.

[19] Zhang, H.G., Tang, S.Y., Yue, H.R., Wu, K.J., Zhu, Y.M., Liu, C., Liang, B., Li, C. (2021). Comparison of computational fluid dynamic simulation of a stirred tank with polyhedral and tetrahedral meshes. *Iranian Journal of Chemistry & Chemical Engineering-International English Edition*, Vol.39(4), pp.311-319.

[20] Zhu, Y., Cai, H., Song, L.B., Wang, X.W., Shang, Z.H., Sun, Y.N. (2020). Aerated irrigation of different irrigation levels and subsurface dripper depths affects fruit yield, quality and water use efficiency of greenhouse tomato. *Sustainability*, Vol.12(7), pp. 2703.